Environmental Science and Pollution Research
https://doi.org/10.1007/s11356-020-10160-0

RESEARCH ARTICLE

Toward the reduction of water consumption in the vegetable-processing industry through membrane technology: case study of a carrot-processing plant

Céline Garnier[1] · Wafa Guiga[1,2] · Marie-Laure Lameloise[1] · Laure Degrand[1,2] · Claire Fargues[1,3]

Received: 3 January 2020 / Accepted: 16 July 2020

Abstract

The food industry consumes large amounts of clean, potable water and in turn generates a significant amount of wastewater. In order to minimize water consumption, membrane technologies represent a suitable solution for the treatment of wastewater before it is recycled as process water. Many studies have shown the effectiveness of this technology in the dairy industry, but there are few studies in the fruit- and vegetable-processing sectors. A recently developed methodology for the reduction of water consumption was tested here. Compounds to be eliminated were identified through chemical analysis of several wastewater samples from a carrot-peeling process. Drinking-water quality was selected as our target. Total suspended solids (TSS), fructose, glucose and sucrose were identified as key parameters. Salts (particularly Ca^{2+} and Mg^{2+}), pH and carbonate hardness (CH) were identified as indicators for evaluating the risk of scaling and corrosion. Based on these results, sieving followed by a 0.5-μm microfiltration (MF) was chosen as the process for pre-treatment. Four nanofiltration (NF) membranes (NFW from SYNDER, DK from GE, NF270 from DOW and SR3D from KOCH) and three reverse osmosis (RO) membranes (ESPA4 from Nitto Group Company, BW30 from DOW and HRX from KOCH) were then tested for the capacity to minimize chemical oxygen demand (COD) and to principally remove sugars. These membranes were then evaluated in terms of permeability and rejection rates. High-quality water could be obtained with RO membranes at low pressure (up to 15 bar) while limiting fouling risks. Rejection rates up to 98.3, 98.0, 99.2, 99.2 and 99.4% for conductivity, COD, fructose, glucose and sucrose, respectively, were achieved. These results are very encouraging for future reuse in vegetable processing before the blanching step, after an additional disinfection treatment.

Keywords Membrane process · Food industry · Water · Reuse · Water management · Effluent treatment

Introduction

Human activities, and industrial activity in particular, have greatly contributed to the problem of water scarcity. There is an emergent need to take into account the sustainability of selected treatment processes to ensure the renewability of this resource for an ever-increasing world population. The food industry largely depends on water, and in most cases drinking water (Casani et al. 2005), the latter representing 75% of the water consumed in this sector in the European Union (EU) (Valta et al. 2016). The French National Research program ANR MINIMEAU (ANR-17-CE10-0015) currently aims to investigate the possibilities of reusing and recycling wastewater in the French agro-food sector by developing an integrated approach combining water footprint assessment and mass pinch analysis (Nemati-Amirkolaii et al. 2019). In this project, selected effluents were to be withdrawn from the conventional wastewater treatment system and treated at the source, utilizing physical-chemical technologies. This involved the development of a generic approach for the choice of treatment solutions, in relation to effluent composition and targeted quality. A French factory producing frozen carrots was selected for

Responsible editor: Angeles Blanco

✉ Claire Fargues
claire.fargues@agroparistech.fr

[1] Université Paris-Saclay, INRAE, AgroParisTech, UMR SayFood, 91300 Massy, France

[2] Conservatoire National des Arts et Métiers, 75003 Paris, France

[3] AgroParisTech, 1 avenue des Olympiades, 91744 Massy Cedex, France

JnlID 11356_ArtID 10160_Proof# 1 - 21/07/2020

a first case study. The objectives were first to determine the key parameters that define wastewaters from carrot-peeling and blanching operations, and develop a treatment process that would be easy to implement locally; second, and more importantly, to contribute to the water sobriety challenge facing society, by promoting internal loops for water reuse in agro-food industries and offering recommendations and rules for the implementation of treatment processes.

This type of industry is characterized by high water consumption and consequently high discharge levels: according to Siddiq and Uebersax (2018), they can reach 12 m^3 of wastewater, with 20 kg biochemical oxygen demand (BOD) and 12 kg total suspended solids (TSS) per ton of processed product. In existing processing plants, water consumption and discharges may vary from these values, depending on the amount and variety of raw vegetable matter and the manufacturing process itself. Moreover, due to seasonality, several vegetable types are generally treated on the same production line. Lehto et al. (2014) report that in processing plants treating four different types of vegetables (lettuce, carrots, potatoes and another root vegetable), water consumption can vary from 1.5 to 5.0 m^3 t^{-1} for the final product.

In Lehto's study, wastewaters were characterized with global parameters, which is not sufficient to select and design a recycling process (Garnier et al. 2019). For instance, organic matter (OM) is usually quantified through chemical oxygen demand (COD) and BOD. Yet, whatever the nature of the pollutants—dissolved or not, settleable or not—removal treatment processes will be very different (Kern et al. 2006). For example, a coagulation treatment will be inefficient for OM removal in carrot-treatment wastewaters, due to the high proportion of carbohydrates present, which are resistant to this type of physicochemical treatment.

Moreover, Lehto et al. (2014) showed that almost 90% of the total water used in a carrot-processing plant was for washing (soil removal) and rinsing (after peeling) operations, which produced more than 90% of the organic load in dissolved form (after peeling with abrasives and peeling machines). The authors also indicated that if peeling wastewater could be treated separately, other wastewaters could be reused and treated more easily. For this reason, many authors recommend considering each wastewater flow separately for reuse or recycling, before mixing and transfer to a wastewater treatment plant (Kern et al. 2006; Lehto et al. 2014; Siddiq and Uebersax 2018, Mundi 2013, Mundi and Zytner 2015).

The most common treatment processes reported in the literature are sedimentation, precipitation with chemicals, centrifugation, dissolved air flotation (DAF), microfiltration (MF) and biological treatment. Lehto et al. (2014) reported that sedimentation of carrot-peeling wastewater can allow TSS and COD to be reduced by at least 77% and 27%, respectively. The addition of chemicals (0.05% ferrisulphate and polyaluminium chloride) led to an extra OM precipitation of 20 to 25%. When wastewaters from washing operations were treated with the addition of chemicals, COD reduction reached 80%. However, for effluents from fresh-cut fruit and vegetable industries, Mundi and Zytner (2015) reported that sedimentation with coagulation and flocculation was less effective for the removal of solids, compared to centrifugation and DAF, due to the high dosages of alum and ferric chloride needed. For water reuse, these authors recommend DAF followed by MF (2 μm and 0.2 μm) which results in a turbidity level below 2 NTU, and even down to 0.02 NTU, depending on the effluent source. But no information is given on the remaining OM in the water to be reused. Other studies (Ardley et al. 2019; Kern et al. 2006; Lehto et al. 2014) have shown that biological processes, in particular sequencing batch reactor (SBR) treatment, were efficient for the removal of OM from peeling wastewaters due to the high biodegradability of the free sugars. For wastewater from the peeling of carrots, onions and beetroots together, a biological treatment (with ferrosulphate and caustic soda) followed by three sedimentation steps and equalization led to purified water with the following characteristics: $BOD_7 = 9.8$ mg O_2 L^{-1} (99–100% removal), COD = 104 mg O_2 L^{-1} (98% removal), total P = 0.8 mg L^{-1} (95% removal), total N = 4.0 mg L^{-1} (94% removal) and TSS = 35 mg L^{-1} (97% removal) (Lehto et al. 2009). However, the quality achieved was still insufficient for reuse purposes, and therefore, additional treatment would be required.

Membrane technologies are more and more frequently used for the production of drinking-quality water from domestic and industrial wastewater (Warsinger et al. 2018) and represent a relevant solution in many cases in food industries (Klemes et al. 2008; Lens et al. 2002). They are appreciated for their high efficiency, disinfection ability and flexibility. Submerged MF on flat polyvinylidene fluoride (PVDF) membranes with a nominal pore size of 0.2 μm was shown to be a cheap (Warsinger et al. 2018) and efficient step in the treatment of fresh-cut vegetable wastewater (peeled baby carrots, shredded lettuce, raw vegetable salads and other vegetables) containing free chlorine (Nelson et al. 2007). The authors stated that the permeate could be reused as cleaning water in the preliminary soil removal step. Ceramic ultrafiltration membranes made of silicon carbide with a 0.05- or 0.1-μm cut-off, followed by a spiral-wound polyamide reverse osmosis (RO) membrane (the SW30HR or the TW30) were tested to treat carrot washing water (Reimann 2002). The quality of the permeate was consistent with the minimum requirements of the German regulations for reuse in 2002. In that case, membrane fouling (MF to RO) with carrot processing wastewater was observed and should be considered (Nelson et al. 2007; Reimann 2002). Even when ultrafiltration was used in pre-treatment, a decrease of RO membrane permeability and COD selectivity was observed over a 2-h period before stabilization (Reimann 2002).

Considering that the focus of the project was on the design of a treatment solution that could quickly be implemented locally, membrane treatments were selected, and only commercially available techniques and membranes were considered. As an initial analysis of the effluent is essential for the selection of an appropriate treatment, the first step consists of creating an effective procedure to analyse carrot wastewaters. In particular, attention was focused on carbohydrates which are present at about 10% (w/w) in carrots (Sharma et al. 2012), and more precisely on sucrose, glucose and fructose which represent about half of the carbohydrate content and are highly water soluble (according to the USDA Nutrient Database). After an adequate pre-treatment, several NF and RO membranes were tested. Warsinger et al. (2018) indicated that several challenges remained for membrane use for potable water reuse which were in particular (i) improving membrane permeability to water, (ii) predicting and preventing membrane fouling and (iii) improving rejection of the remaining contaminants. Therefore, after determination of the membrane permeability for four NF membranes and three RO membranes, the critical flux is established in order to prevent membrane fouling, and the rejection of COD, sugars (glucose, fructose and sucrose) and salts is discussed.

Materials and methods

Wastewater sources

Wastewater was obtained from a French factory producing different varieties of frozen vegetables and selected by the Technical Centre for Food Product Conservation (CTCPA, Paris, France). For carrot processing presented in Fig. 1, effluents are produced following several of the unit operations, and in particular the peeling and rinsing step and the blanching step. As the peeling and rinsing process is responsible for one third of the water consumption, wastewater from carrot peeling was selected for the first case study, in accordance with CTCPA.

Several peeling techniques exist, utilizing blades (peeling machine), abrasion, steam-facilitated abrasion, caustic treatment and flame peeling (European Union 2018). Here steam-facilitated abrasion was used, leading to water consumption up to five times more than with caustic treatment, but half that of a combination of abrasion and machine peeling (European Union 2018).

Wastewater from blanching was also analysed in order to confirm the selection of specific compounds to be eliminated (i.e. key parameters). As drinking water was used at each step of the carrot processing operation, it was also sampled for analysis in order to verify the origin of wastewater ions.

All samples were kept frozen at − 18 °C. They were then thawed at ambient temperature for approximately 48 h before analyses and treatments.

Analytical methods

The following analyses were performed on all raw wastewaters from the processing units, pre-treated wastewater from peeling and rinsing, and treated wastewater from peeling and rinsing:

- Global parameters: TSS, particulate and dissolved COD, conductivity, pH, turbidity and CH
- Dissolved organic pollution: glucose, fructose and sucrose
- Free and total chlorine
- Ionic compounds: chlorides, nitrites, nitrates, phosphates, sulphates, sodium, ammonium, potassium, magnesium and calcium

High-performance ion-exchange chromatography (HPIC) was carried out using a Dionex ICS-5000+ system (ThermoFisher Scientific, Waltham, MA, USA) for anions and sugars and a Dionex ICS-2000 system (ThermoFisher Scientific) for cations, both equipped with the same AS-AP autosampler, and using the suitable operating conditions for each analysis, summarized in Table 1. Mixtures of mono- and disaccharides (glucose, fructose and sucrose), as well as mixtures of anions and mixtures of cations, were diluted in water and used as external standards. The Chromeleon Chromatography Data System (version: 6.08 SR15b Build 4981, ThermoFisher Scientific) was used for data acquisition and processing. Concerning chemicals, eluent for IC (50% NaOH in water, 0.1 M Na_2CO_3, 0.1 M $NaHCO_3$ and 0.1 M CH_4O_3S) and TraceCERT ® materials for IC (anions, cations, glucose, fructose and sucrose) were purchased from Sigma-Aldrich (St Louis, USA). All aqueous solutions were prepared with ultrapure water obtained from the Purelab flex water purification system (Veolia Water Solutions and Technologies, Saint-Maurice, France).

TSS analysis followed the requirements of standard methodology (NF EN 872).

COD, CH and chlorine levels (free and total) were determined with rapid test-tube and photometric measurements (Nanocolor 400D - Macherey Nagel, Hoerdt, France). Concerning COD, sample oxidation was performed with a potassium dichromate–sulphuric acid–silver sulphate method at 148 °C for a duration of 2 h (error ± 3%). Dissolved COD was measured after sample filtration at 0.45 μm.

The measured content of the sugars present allowed an equivalent COD for sugars to be calculated, and labelled COD_{sugars}. When possible, additional OM was quantified through a differential COD for pre-treated effluents, defined as

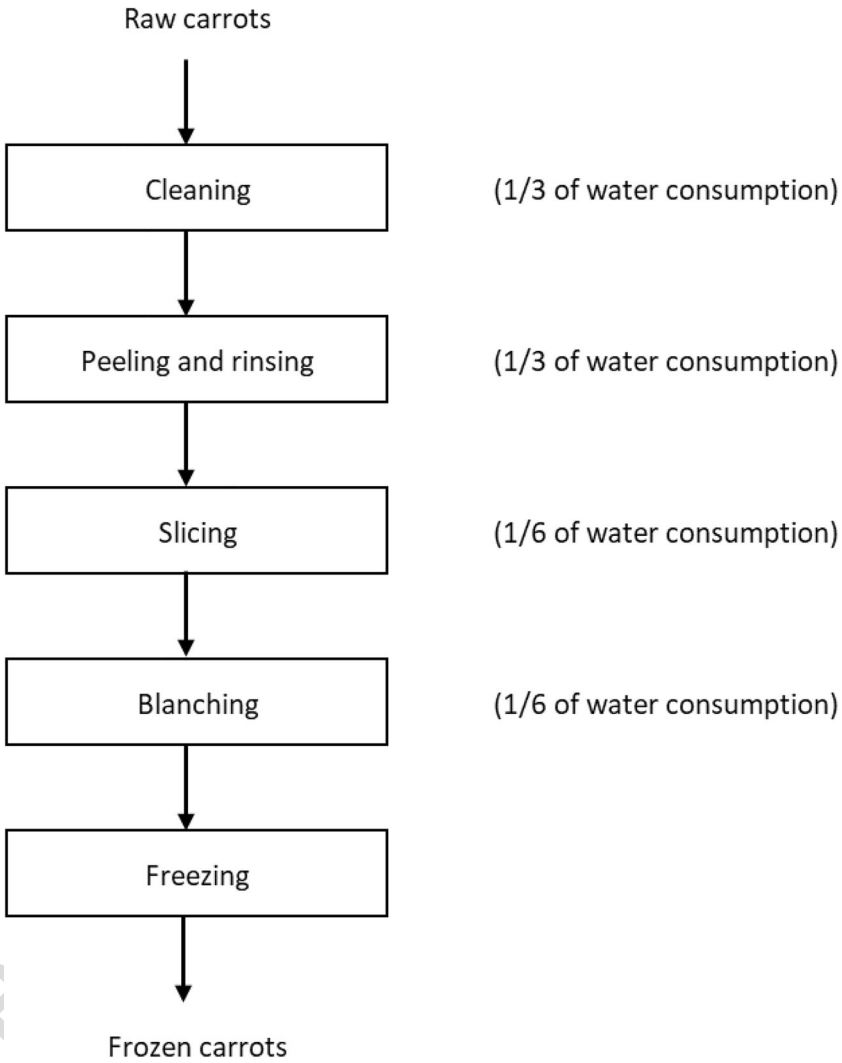

Fig. 1 Schematic representation of carrot processing operation

$$COD_{diff} = COD - COD_{sugars}$$

As membranes have limited chlorine tolerances, free and total chlorine were measured to ensure that there was no risk of membrane damage.

Electrical conductivity (error ± 0.5%, referenced at 20 °C) and pH (error ± 0.01) were monitored at ambient temperature. Turbidity was measured by a turbidity meter, model 2100 AN (Hach, France) with an accuracy of ± 2%.

UV spectrophotometry (between 200 and 400 nm) and optical density measurement at about 215 nm (OD_{215}) allowed the presence of amino acids and peptides in some of the samples to be globally evaluated.

Pre-treatment

In order to select an appropriate wastewater pre-treatment, the following operations were tested in series in dead-end filtration mode: sieves of successively 169 μm and 79 μm mesh size and filtration at 49 μm and 30 μm, followed by MF with a 1.6-μm cut-off. Given the performances obtained, pre-treatment through sieving at successively 169 μm and 79 μm, followed by MF with a 0.5-μm cut-off was selected.

Membrane fouling control was carried out with the silt density index measurement (SDI) after each filtration step. For SDI tests, effluents were filtered through a 0.45-μm cellulose acetate filter in dead-end filtration mode at 2.1 bar (ASTM Standard D4189).

Particle size distribution of the initial wastewater and of the filtrates was investigated using a laser diffraction particle size analyser (Mastersizer 2000, Malvern Panalytical, UK), allowing for D43 (determining the mean diameter over volume, the DeBroukere mean) and D32 (volume/surface mean, the Sauter mean) to then be calculated.

Membranes

Four NF and three RO membranes were tested (Table 2). Due to the presence of sucrose and glucose/fructose with

t1.1 **Table 1** Selected configurations of HPIC

t1.2		Anions	Cations	Sugars
t1.3	Column	Dionex IonPac™ AS22 Analytical (4 × 250 mm) with a AG22 (4 × 50 mm) guard column (ThermoFisher Scientific)	Dionex IonPac™ CS12A Analytical (4 × 250 mm) with a CG12A (4 × 50 mm) guard column (ThermoFisher Scientific)	Dionex CarboPac™ PA1 Analytical (4 × 250 mm) with a PA-1 guard column (ThermoFisher Scientific)
t1.4	Eluent	4.5 mM Na_2CO_3/1.4 mM $NaHCO_3$	20 mM CH_4O_3S	200 mM NaOH
t1.5	Flow rate	1.2 mL min^{-1}	1.0 mL min^{-1}	1.0 mL min^{-1}
t1.6	Temperature	30 °C	Ambient temperature	Ambient temperature
t1.7	Detection	Suppressed conductivity ASRS™ 300 4 mm Applied current, 31 mA	Suppressed conductivity CSRS™ 300 4 mm Applied current, 59 mA	Pulsed electrochemical detection, gold working electrode, Ag/AgCl reference electrode, pulsed amperometry, quadruple potential waveform
t1.8	Injection volume	25 μL	25 μL	25 μL

respective molecular weights (MW) of 342.3 g mol^{-1} (Stokes diameter = 0.92 nm) and 180.16 g mol^{-1} (Stokes diameter = 0.73 nm) in the carrot-peeling process wastewater, NF membranes with a molecular weight cut-off (MWCO) between 150 and 500 g mol^{-1} were selected. For all the membranes, manufacturers recommend that the feed be dechlorinated and that the SDI be < 5.

After delivery, membranes were stored dry at 4 °C. Before experiments, and in order to remove the protective coating or solution, membranes were dipped in a 0.4 g L^{-1} KOH solution for 2 h and then in deionized water for a minimum of 24 h.

Membrane setup and operating conditions

Experiments were run using a LabStak M20 filtration device from Alfa Laval, France (Fig. 2) allowing several flat-sheet membranes to be tested simultaneously. Each tested membrane has a separate permeate outlet. The retentate outlet is common for all membranes.

The effective area for each membrane was 2 × 0.018 m^2, and the initial wastewater feed volume was approximately 30 L.

The feed tank and main parts of the pilot were of stainless steel in order to limit artefact adsorption.

A new membrane was used for each experiment, which consisted of three steps: deionized water filtration for 2 h maximum, then wastewater filtration for 4 h maximum, and finally (after rinsing) deionized water filtration again. For all experiments, retentate flow rate was set at 300 L h^{-1}; temperature was kept constant at 20 °C (jacketed tank); and transmembrane pressure (TMP) was increased incrementally from 5 to 30 bar (5, 10, 15, 20 and 30 bar). The experiments were run in total recirculation mode: both permeate and retentate were recycled into the feed tank. Sampling and measurements were made after a minimum filtration time of 10 min.

Filtration tests with deionized water were conducted to determine the permeability of pure water (A in L h^{-1} m^{-2} bar^{-1}) of the membrane before and after wastewater filtration. According to Darcy's law, pure water flux (J_w in L h^{-1} m^{-2}) is proportional to TMP (in bars) according to:

$$J_w = A \times \mathrm{TMP} \quad (1)$$

$$J_w = \frac{Q_p}{S} \quad (2)$$

$$\mathrm{TMP} = \frac{P_f + P_r}{2} - P_p \quad (3)$$

with:

Q_p	Permeate flow rate (L h^{-1}) experimentally established by plotting
S	Effective membrane area (m^2)
P_f, P_r and P_p	Feed, retentate and permeate pressures, respectively (bars)

Filtrations were performed on solutions in order to study the influence of TMP on permeate flux and solute (COD, sugars, ions) rejections. When the solution is diluted and in the absence of irreversible fouling, permeate flux (J_p in L h^{-1} m^{-2}) is proportional to the effective TMP (TMP − Δπ) (in bars) according to:

$$J_p = A \times (\mathrm{TMP} - \Delta\pi) \quad (4)$$

$$J_p = \frac{Q_p}{S} \quad (5)$$

$$\Delta\pi = \pi_{r,m} - \pi_{p,m} \quad (6)$$

with:

Δπ	Difference of osmotic pressure (bars)
$\pi_{r,m}$	Osmotic pressure at the membrane interface in the retentate (bars)

$\pi_{p,m}$ Osmotic pressure at the membrane interface in the permeate (bars)

If the osmotic pressures are calculated at the membrane, they take into account the reversible concentration polarization phenomenon (Aimar et al. 2010).

For diluted solutions, osmotic pressure of solute i (π_i in bars) can be estimated by the Van't Hoff relation:

$$\pi_i = C_i \times R \times T \quad (7)$$

with:

C_i Concentration of solute i (mol m^{-3})
R Gas constant (m^3 bar K^{-1} mol^{-1})
T Temperature (K)

The observed rejection of solute i (Tr_i) was calculated with the concentration of solute i in the permeate ($C_{p,i}$ in mg L^{-1}) and in the retentate ($C_{r,i}$ in mg L^{-1}) according to

$$Tr_i = \frac{C_{r,i} - C_{p,i}}{C_{r,i}} \quad (8)$$

Results and discussion

Characteristics of raw wastewater

Table 3 sums up the detailed composition of the processing plant's drinking water and of the different effluents. Composition of the wastewaters strongly varies over time, with COD values lying between 22 and 4730 mg O_2 L^{-1}. This is consistent with a report from the European Union (2018) which identified a COD variation between 18 and 5402 mg O_2 L^{-1} in effluents from fruit and vegetable industries.

Wastewater from the peeling machine

For wastewater from the peeling machine, Lehto et al. (2014) measured a COD between 9.0 and 39.0 g L^{-1} which is significantly higher than the present values and can be explained by the

t2.1 **Table 2** Overview of membrane characteristics according to manufacturer's data

t2.2 Supplier	Membrane	Type	Rejection	MWCO	Active layer polymer	Maximum temperature	Maximum pressure
t2.3 Synder filtration (Vacaville, USA)	NFW	NF	97% 2000 ppm $MgSO_4$ (7.6 bar and 25 °C)	300–500 g mol^{-1}	Semi-aromatic polypiperazine amide	50 °C	41.4 bar if temperature is less than 35 °C Otherwise, 30 bar
t2.4			20% 2000 ppm NaCl (7.6 bar and 25 °C)				
t2.5			98.5% Solution of lactose at 2% (7.6 bar and 25 °C)				
t2.6 GE water and process technologies (Saint-Thibault-des-Vignes, France)	DK	NF	98% 2000 ppm $MgSO_4$ (7.6 bar and 25 °C)	150–300 g mol^{-1}	Semi-aromatic polypiperazine amide	50 °C	41.4 bar if temperature is less than 35 °C Otherwise, 30 bar
t2.7 DOW France (Saint-Denis, France)	NF270	NF	97% 2000 ppm $MgSO_4$ (4.8 bar and 25 °C)	150–300 g mol^{-1}	Semi-aromatic polypiperazine amide	45 °C	41 bar
t2.8 Koch Membrane Systems Division (Lyon, France)	SR3D	NF	> 99.0% 5000 ppm $MgSO_4$ (6.5 bar and 25 °C)	200 g mol^{-1}	Proprietary thin-film composite polyamide	50 °C	44.8 bar
t2.9 Hydranautics – Nitto France (Roissy, France)	ESPA4	RO	99.2% (99.0% minimum)1500 ppm NaCl (10.3 bar and 25 °C)	–	Polyamide thin-film composite	45 °C	40 bar
t2.10 DOW France (Saint-Denis, France)	BW30	RO	99.5% 2000 ppm NaCl (15.5 bar and 25 °C)	–	Polyamide thin-film composite	45 °C	41 bar
t2.11 Koch Membrane Systems Division (Lyon, France)	HRX	RO	99.6% NaCl	–	Proprietary thin-film composite polyamide	50 °C	44.8 bar

Q3 **Fig. 2** Scheme of the LabStak M20 system (Sagne et al. 2008)

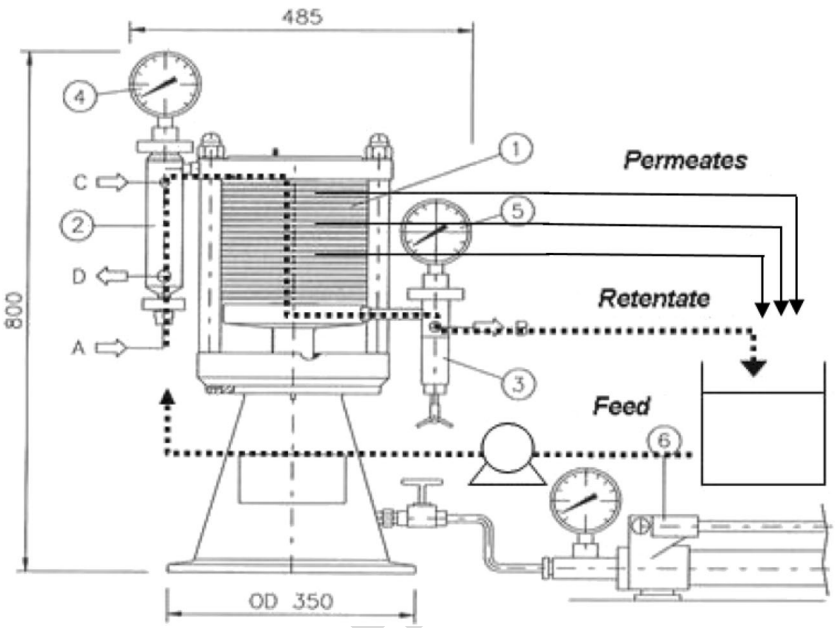

t3.1 **Table 3** Characteristics of factory drinking water and the different raw wastewaters

t3.2	Parameter	Drinking water at the factory	Peeling and rinsing effluent (over a period of 30 min)	Value at the outlet of blanching operation	Value in carrot (as per USDA*)
t3.3	Temperature	n.d.	31 °C	64–71 °C	n.i.
t3.4	TSS	n.d.	20–744 mg L^{-1}	n.d.	n.i.
t3.5	Total COD	3.8 mg O_2 L^{-1}	22–4730 mg O_2 L^{-1}	4403 mg O_2 L^{-1}	n.i.
t3.6	Dissolved COD	n.d.	22–1654 mg O_2 L^{-1}	4064 mg O_2 L^{-1}	n.i.
t3.7	BOD_5 (**)	n.d.	790 mg L^{-1}	n.d.	n.i.
t3.8	TOC (**)	n.d.	432 mg L^{-1}	n.d.	n.i.
t3.9	Conductivity	261 µS cm^{-1}	50–930 µS cm^{-1}	1269 µS cm^{-1}	n.i.
t3.10	pH	6.86	4.97–8.40	7.24	n.i.
t3.11	Turbidity	< 0.1 NTU	6–385 NTU	34.7 NTU	n.i.
t3.12	CH	3.5°f	5.9–12.9°f	19.6°f	n.i.
t3.13	Fructose	without	1–151 mg L^{-1}	210 mg L^{-1}	0.55 g/100 g
t3.14	Glucose	without	0–187 mg L^{-1}	280 mg L^{-1}	0.59 g/100 g
t3.15	Sucrose	without	10–663 mg L^{-1}	3010 mg L^{-1}	3.59 g/100 g
t3.16	Chlorides (Cl^-)	42 mg L^{-1}	46–72 mg L^{-1}	167 mg L^{-1}	n.i.
t3.17	Nitrites (NO_2^-)	< LD	< LD	< LQ	n.i.
t3.18	Nitrates (NO_3^-)	5 mg L^{-1}	6–8 mg L^{-1}	16 mg L^{-1}	n.i.
t3.19	Phosphates (PO_4^{3-})	< LD	0–8 mg L^{-1}	36 mg L^{-1}	Phosphorus: 35 mg/ 100 mg
t3.20	Sulphates (SO_4^{2-})	15 mg L^{-1}	16–22 mg L^{-1}	33 mg L^{-1}	n.i.
t3.21	Sodium (Na^+)	19 mg L^{-1}	17–27 mg L^{-1}	56 mg L^{-1}	69 mg/ 100 g
t3.22	Ammonium (NH_4^+)	< LD	0–1.5 mg L^{-1}	3 mg L^{-1}	n.i.
t3.23	Potassium (K^+)	4 mg L^{-1}	5–113 mg L^{-1}	281 mg L^{-1}	320 mg/100 g
t3.24	Magnesium (Mg^{2+})	6 mg L^{-1}	6–10 mg L^{-1}	8 mg L^{-1}	12 mg/100 g
t3.25	Calcium (Ca^{2+})	22 mg L^{-1}	32–52 mg L^{-1}	41 mg L^{-1}	33 mg/100 g
t3.26	Endosulfan sulphate, fenitrothion, malathion, parathion-methyl, chlorpyrifos, ethion, bromophos-ethyl, chlorfenvinphos, chlorpyrifos-methyl, diazinon, ethyl parathion, bromophos-methyl, prometryne (**)	n.d.	< 0.05 µg L^{-1}	n.d.	n.d.
t3.27	Endosulfan (total), endosulfan alpha, beta-endosulfan, chlorpyrifos (**)	n.d.	< 0.02 µg L^{-1}	n.d.	n.d.
t3.28	Dichlorvos (**)	n.d.	< 0.11 µg L^{-1}	n.d.	n.d.
t3.29	Malathion (**)	n.d.	< 0.100 µg L^{-1}	n.d.	n.d.
t3.30	Linuron (**)	n.d.	< 0.025 µg L^{-1}	n.d.	n.d.

n.i. not indicated, *n.d.* not determined

*https://fdc.nal.usda.gov/fdc-app.html#/food-details/170393/nutrients published 4/1/2019

**One analysis done by an external laboratory

t4.1 **Table 4** Example of particle size distribution after several pre-treatments

t4.2		Raw wastewater	Wastewater pre-treated at 169 μm	Wastewater pre-treated at 79 μm	Wastewater pre-treated at 0.5 μm
t4.3	D43 (μm)	591	194	108	n.d.
t4.4	D32 (μm)	148	60	47	n.d.

n.d. not determined

abrasive and machine peeling mode used in their study. Furthermore, the wastewater studied here is a mix of peeling and rinsing water.

Wastewater from the peeling operation is gathered in the condensed stream from the initial peeling step, but wastewater from the subsequent rinsing is also collected, resulting in average temperatures of up to 31 °C. It contains TSS (peelings), dissolved substances such as sugars (fructose, glucose and sucrose) and ions including mainly chlorides, sulphates, sodium, potassium and calcium (Table 3). Sugars are the major identified compounds and represent between 36 and 67% of the total COD and between 51 and 92% in its dissolved form. With $COD_{tot}/BOD_5 = 2.1$, this effluent is therefore highly biodegradable (Truc 2007). Studies are underway to more accurately identify the additional dissolved substances, especially peptides and amino acids present in carrots and detected by UV spectrophotometry in the effluent (OD_{215} between 2 and 2.5). According to the USDA Nutrient Database, glutamic acid, threonine, aspartic acid, alanine, leucine and lysine, with molecular weights between 80 and 150 g mol^{-1}, are the main amino acids present in carrots. No pesticides were detected, probably because carrot roots are less exposed than their above-ground parts; they could also have been eliminated with residual soil during the cleaning process.

Wastewater from the blanching operation

Wastewater from the blanching operation contains the same components as the peeling wastewater, but at higher concentrations. Blanching consists of bringing the carrots to a high temperature for a short period of time in order to inactivate or retard bacterial growth and enzyme action. It uses hot water at 80 to 100 °C, or steam, and leads to wastewater temperatures between 64 and 71 °C. This results in an increase in sugar solubility and diffusion (more than 40% for sucrose between 30 and 65 °C) (Macedo 2005) and explains their higher concentration and COD levels.

Selection of key parameters and other indicators

In order to identify the origin of the compounds in the effluent, the composition of wastewater was compared to that from standard carrot-processing procedures, as well as with drinking water from the processing plant (Table 3). Higher concentrations of minerals in wastewater confirm their transfer from carrots during peeling. For instance, wastewater contains up to 95 mg L^{-1} of K^+, whereas drinking water contains only 4 mg L^{-1}; this can be explained by the elevated presence of this element in carrots: 320 mg/100 g. With respect to sugars, equivalent amounts of fructose and glucose are found in carrots, while the level of sucrose is 8 times as high. In the wastewater produced, the proportions of fructose and glucose are respected, and even if its presence is 8 times that of fructose and glucose, it would appear that sucrose tends to transfer to a much lesser extent. A possible explanation could be hydrolysis into fructose and glucose.

According to the methodology developed in the ANR MINIMEAU to reduce water consumption, key parameters (specific compounds to be eliminated) have to be selected (Garnier et al. 2019). The production of water of drinking quality requires the elimination of TSS and the reduction of the COD figures. Fructose, glucose and sucrose are the major components of this effluent and may provoke rapid bacterial

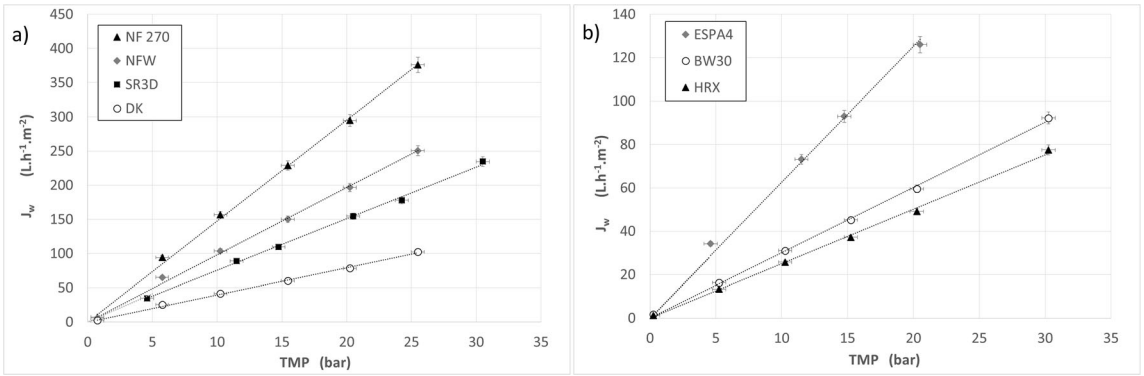

Fig. 3 Pure water permeate flux (20 °C, feed flow rate = 300 L h^{-1}): **a** NF membranes and **b** RO membranes

JrnlID 11356_ArtID 10160_Proof# 1 - 21/07/2020

t5.1 **Table 5** Pure water permeability before and after treatment, in comparison with existing literature data

t5.2 Supplier	Membrane	Type	Pure water permeability measured at 20 °C (in L h^{-1} m^{-2} bar^{-1})		Pure water permeability reported by other authors (normalized at 20 °C)	
t5.3			Before effluent filtration	After effluent filtration (percentage decrease from initial permeability)	Pure water permeability (on flat sheet, L h^{-1} m^{-2} bar^{-1})	References
t5.4 DOW France	NF270	NF	14.8	11.4 (− 23%)	13.5	Racar et al. 2017
t5.5					12.0	Nguyen et al. 2015
t5.6 Synder Filtration	NFW	NF	9.8	8.6 (− 12%)	4.8	Zhao et al. 2015
t5.7					4.0	Yuan et al. 2018
t5.8 Koch Membrane Systems Division	SR3D	NF	7.5	5.6 (− 25%)	No data found	–
t5.9 GE Water & Process Technologies	DK	NF	4.0	4.1 (0%)	4.2	Negaresh et al. 2012
t5.10					6.1	Nguyen et al. 2015
t5.11 Hydranautics	ESPA4	RO	6.3	4.7 (− 25%)	6.5	Richards et al. 2010
t5.12 DOW France	BW30	RO	3.0	3.1 (0%)	2.4	Balannec et al. 2005
t5.13					3.4	Richards et al. 2010
t5.14 Koch Membrane Systems Division	HRX	RO	2.5	2.6 (0%)	No data found	–

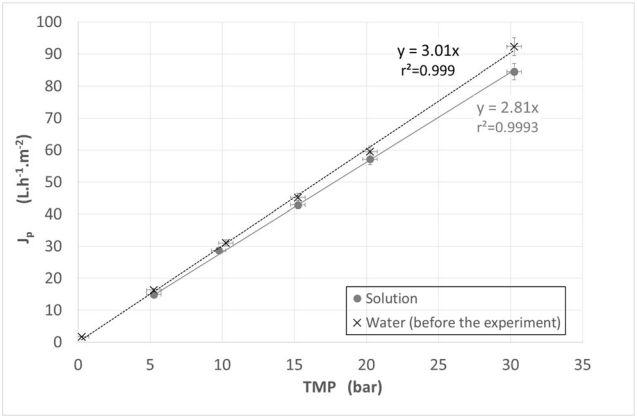

Fig. 4 Permeate flux for pure water and solution, using the BW30 membrane

growth. As disinfection of wastewater is a priority in the fruit and vegetable industries (Manzocco et al. 2015), their removal constitutes a primary objective. TSS, COD, fructose, glucose and sucrose were therefore chosen as key parameters.

As mineral concentrations are lower in wastewater than in drinking water, they do not appear as key parameters for the treatment process evaluation, but they represent essential indicators that have to be monitored at each step of the treatment scheme. In fact, it was shown that they can affect the rejection rate of organic solutes through modification of membrane properties (pore swelling, electrical charge, etc.) or even through the molecular radius of the different solutes (Galier et al. 2013; Mohammad et al. 2010). Moreover, with respect to pH and CH control, they provide an overview of the water's state of equilibrium, and thus a basis for evaluating the risk of scaling or corrosion. For example, scaling near the membrane can cause fouling (Aimar et al. 2010).

Pre-treatment selection

Pre-treatment operations were selected to comply with manufacturers' recommendations regarding the maximal SDI.

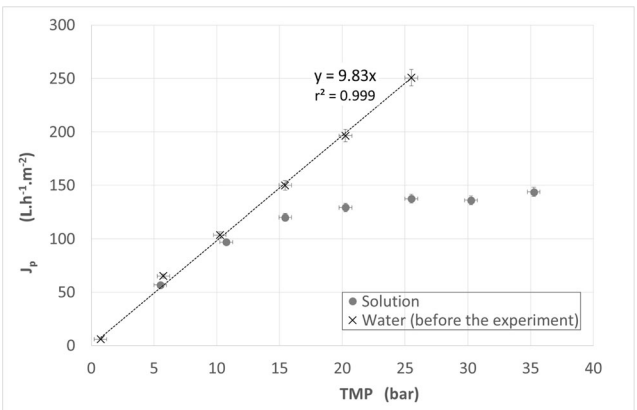

Fig. 5 Permeate flux for pure water and solution, using the NFW membrane

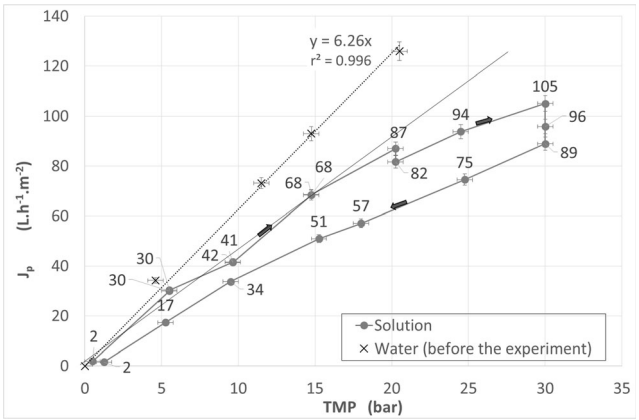

Fig. 6 Permeate flux for pure water and solution using the ESPA4 membrane; hysteresis highlighted

Particles contained in peeling effluents settle very quickly (in less than 2 min), which leads to a reduction in COD of around 22%. In fact, in the EU (European 2018), the largest particles from peeling are generally separated by sedimentation. In this study, sedimentation was replaced by an equivalent sieving step, utilizing microfiltration.

Rapid fouling was observed via SDI tests with the filtrate after sieving from 169 to 30 μm. This is consistent with the particle size analysis of this effluent, revealing a particle size distribution in volume mainly between 30 and 2000 μm and a D43 of about 600 μm (Table 4). These results agreed with those of Nelson et al. (2007) with particle size lying between 0.5 and 1000 μm for fresh-cut vegetable wastewater (shredded lettuce, raw vegetable salad, peeled baby carrots and other vegetables).

SDI was reduced to 17 after MF at 1.6 μm and less than 5 after further filtration at 0.5 μm. It appears essential to microfilter the effluent at 0.5 μm prior to further treatment.

Progressive sieving at 169 μm and 79 μm and dead-end MF at 0.5 μm were then applied as pre-treatment. Sieving leads to a decrease in D43 at successively 194 μm and 108 μm. The removal efficiency of this pre-treatment reaches

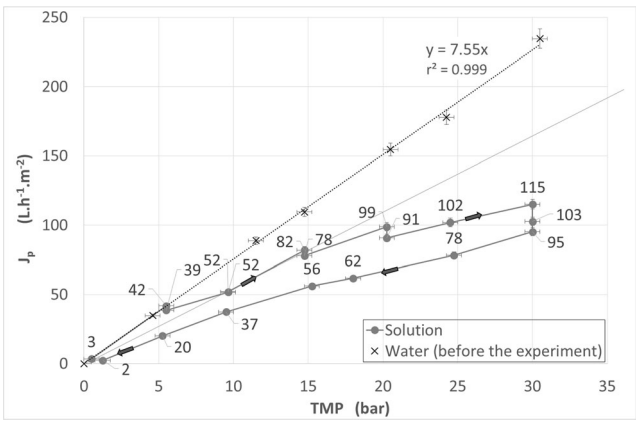

Fig. 7 Permeate flux for pure water and solution using the SR3D membrane; hysteresis highlighted

93% for TSS (89% by sieving at 169 μm) and an average of 28% for COD (26% at 169 μm). COD reduction is lower but consistent with that obtained by Reimann (2002) (between 30 and 40%), where pre-treatment was pushed toward ultrafiltration with a pore diameter of 0.05 or 0.1 μm.

The pre-treated effluent was analysed for its residual pollution: 1–52 mg L^{-1} TSS, 16–3406 mg O_2 L^{-1} COD 50, 930 μS cm^{-1} conductivity, 1–151 mg L^{-1} fructose, 0–187 mg L^{-1} glucose and 10–663 mg L^{-1} sucrose.

Membrane water permeability

Before wastewater treatment, pure water permeability of the selected membranes was studied (Fig. 3). A high linear correlation ($r^2 > 0.991$) between the pure water permeate flux and the TMP was found according to Darcy's law and equation (see Eq. 1). Resulting water permeability values are given in Table 5.

Values of water permeability are consistent with those reported by other authors (Table 5) except for the NFW membrane. Variations in water permeability may be due to differences in filtration module geometry or in compaction procedures (Mohammad et al. 2010; Nguyen et al. 2016).

As expected, RO membranes display lower water permeability than NF, with the exception of ESPA4 (RO) which has higher permeability than DK (NF). Amongst RO membranes, ESPA4 exhibits the highest permeability followed by BW30 and HRX whereas for the NF membranes, NF270 exhibits the highest and DK the lowest permeability.

Critical flux, concentration polarization and fouling

In what follows, "solution" will refer to the pre-treated effluent tested utilizing NF or RO.

Pure water permeability at 20 °C was measured before and after solution treatment, and the corresponding loss of permeability was calculated to evaluate potential fouling (Table 5). Whatever the membrane type, when pure water permeability was initially higher than 4 L h^{-1} m^{-2} bar^{-1}, a loss of water permeability up to 23% was found, showing that with these membranes, fouling had occurred.

Permeate flux for the solution was also measured and compared with initial pure water flux. Two different behaviours were observed: for the less permeable BW30 (Fig. 4) and HRX membranes, the relation between permeate flux and TMP was linear, showing that the critical flux was not reached in this range (Aimar 2006). The DK membrane displayed quite the same behaviour, but only up to 25 bar. Permeate flux was always below that of pure water, with a gap increasing along with TMP, corresponding to a pressure gap of up to 5 bar for the highest fluxes. This highlights a reversible concentration polarization phenomenon (Aimar et al. 2010), not taken into account in these

Table 6 Characteristics of solution before and after contact with the SR3D, ESPA4 and DK membranes

Parameter	Values before contact	Values after contact	Loss (%)
Turbidity	1.1 NTU	1.1 NTU	0%
Total COD	674 mg O_2 L^{-1}	586 mg O_2 L^{-1}	13%
Dissolved COD	679 mg O_2 L^{-1}	589 mg O_2 L^{-1}	13%
Fructose	71.8 mg L^{-1}	66.8 mg L^{-1}	7%
Glucose	66.3 mg L^{-1}	61.5 mg L^{-1}	7%
Sucrose	325 mg L^{-1}	302 mg L^{-1}	7%
COD_{diff}	162 mg L^{-1}	110 mg L^{-1}	32%
Conductivity	468 µS cm^{-1}	430 µS cm^{-1}	8%
pH	7.23	7.35	− 2% (24% in H^+)
Chlorides (Cl^-)	59 mg L^{-1}	49 mg L^{-1}	17%
Nitrates (NO_3^-)	7 mg L^{-1}	6 mg L^{-1}	14%
Phosphates (PO_4^{3-})	4 mg L^{-1}	4 mg L^{-1}	0%
Sulphates (SO_4^{2-})	18 mg L^{-1}	16 mg L^{-1}	11%
Sodium (Na^+)	45 mg L^{-1}	50 mg L^{-1}	− 11%
Potassium (K^+)	56 mg L^{-1}	55 mg L^{-1}	2%
Magnesium (Mg^{2+})	8 mg L^{-1}	8 mg L^{-1}	0%
Calcium (Ca^{2+})	45 mg L^{-1}	50 mg L^{-1}	−11%
Hardness (calculated)	14.6°f	15.8°f	− 9%
CH	9.1°f	8.2°f	10%

figures: in fact, sugars and salts in the solution are responsible for an osmotic pressure of only 0.16 bar (Eq. 7), which could in no way explain the pressure gaps observed (Figs. 4, 6, and 7). This phenomenon was also mentioned by Almazán et al. (2015) during the nanofiltration of glucose: introducing concentration polarization into the

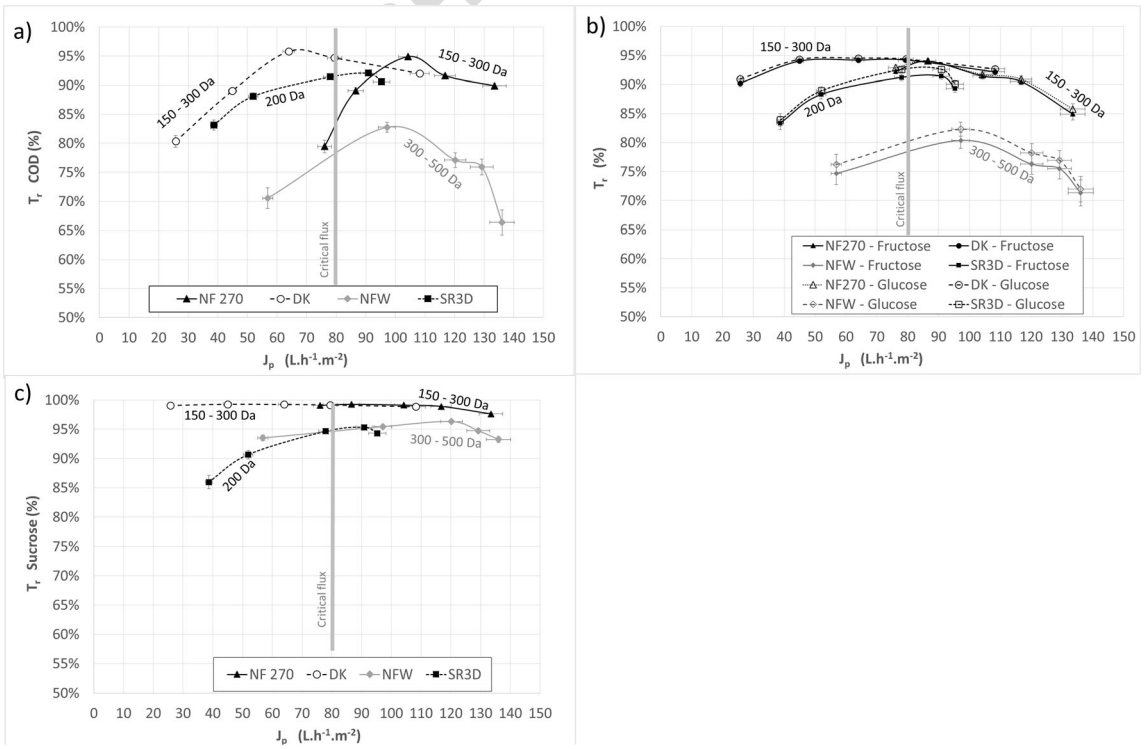

Fig. 8 Rejection of COD and sugars as a function of permeate flux with NF membranes (20 °C, feed flow rate = 300 L h^{-1}): **a** COD, **b** glucose and fructose, **c** sucrose

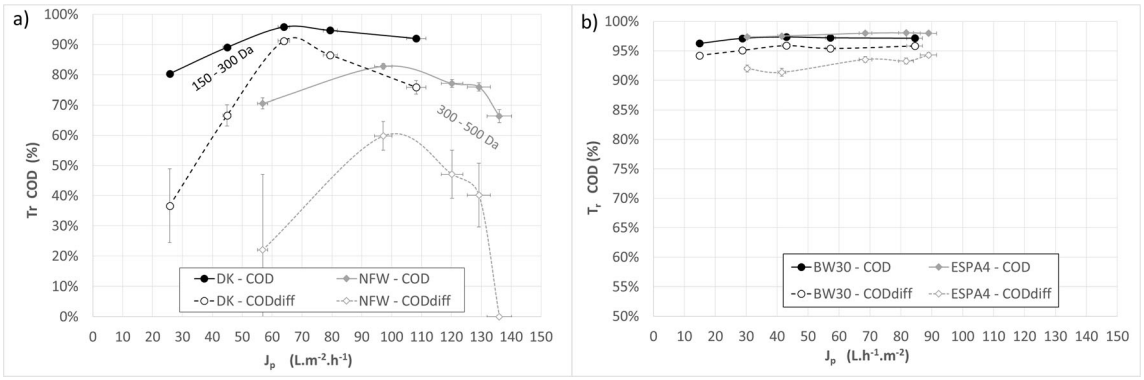

Fig. 9 COD rejections as a function of permeate flux with (20 °C, feed flow rate = 300 L h^{-1}): **a** NF membranes, **b** RO membranes

calculation of osmotic pressure to correct TMP (Eq. 4), they observed that both permeate and pure water flux curves merged.

For membranes with the highest permeability (above 4 L h^{-1} m^{-2}) such as the NFW (Fig. 5), the linearity range was reduced as water permeability increased: it was linear up to 20 bar for ESPA4 and only 5 bar for NF270. When the critical flux is exceeded, irreversible fouling occurs, as was previously observed by the permeability loss of these membranes (Table 5).

For the ESPA4 (Fig. 6) and the SR3D (Fig. 7) membranes (with water permeability of 6.3 and 7.5 L h^{-1} m^{-2} bar^{-1}, respectively), the evolution of permeate flux was studied over time to check the critical flux value. For each pressure applied up to 20 bar, two flux measurements were made, after 5 min (initial flux) and after 30 min of the run; for 30 bar, it was measured after 5, 15 and 30 min. At the lowest pressures, no permeate flux difference was observed with time, showing that no fouling had occurred and that the steady state was quickly reached. For both membranes, the same critical flux of about 80 L h^{-1} m^{-2} was reached at TMP = 18 bar for ESPA4 and TMP = 15 bar for SR3D, above which the permeate flux decreased with time. A decrease of up to 15% for the highest TMP was observed after a 30-min run. This confirms the result of Reimann (2002) who showed that for the RO membrane, flux stabilization occurred only after several hours of run.

When the pressure was further decreased (from 30 to 1 bar), hysteresis appeared for both membranes, consistent with the fact that the critical flow had been exceeded (Aimar et al. 2010).

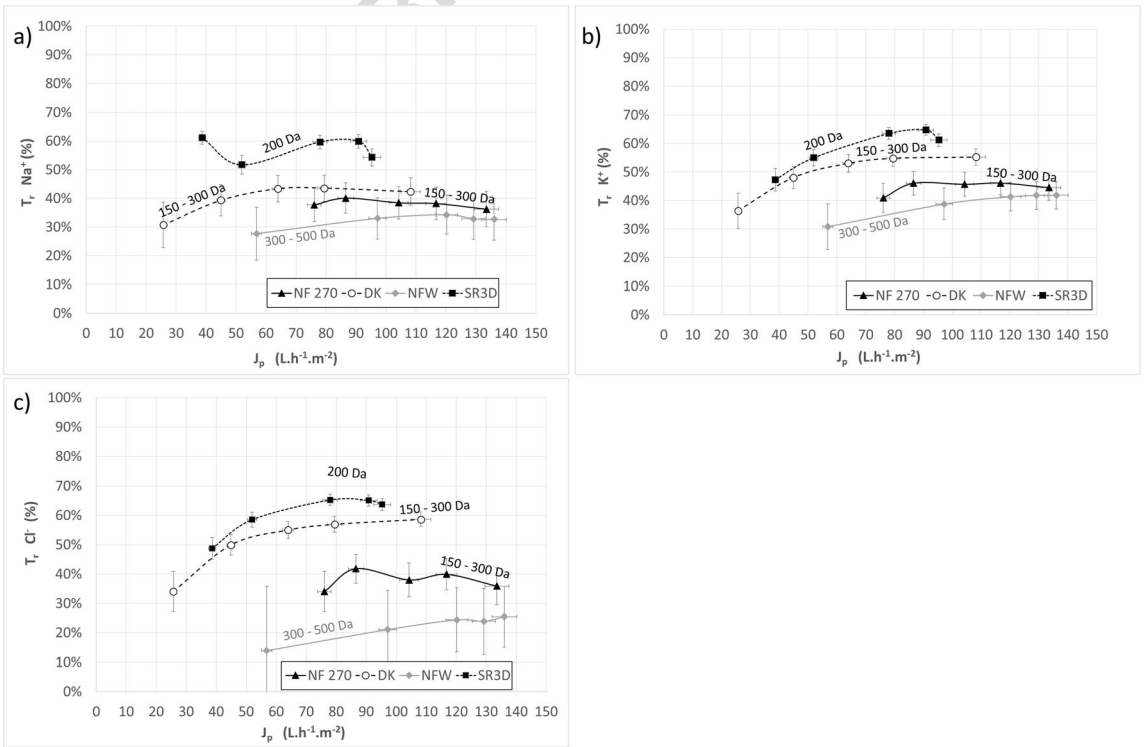

Fig. 10 Monovalent ion rejection as a function of permeate flux with NF membranes (20 °C, feed flow rate = 300 L h^{-1}): **a** Na^+, **b** K^+, **c** Cl^-

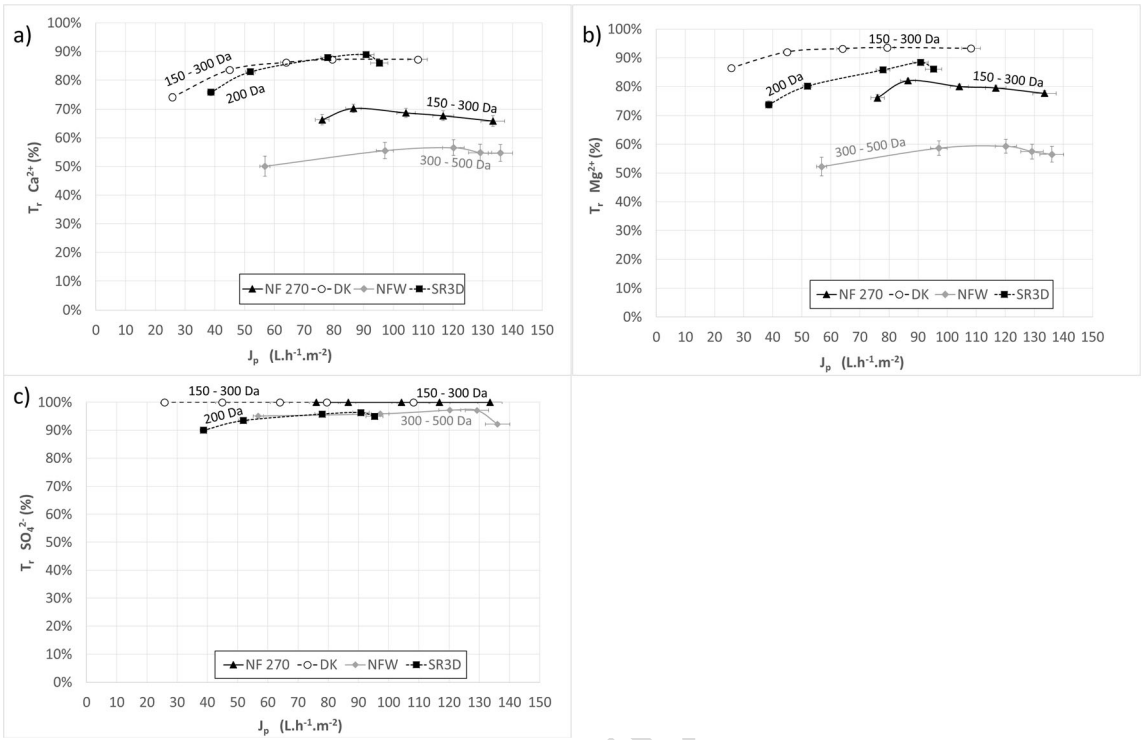

Fig. 11 Divalent ion rejection as function of permeate flux with NF membranes (20 °C, feed flow rate = 300 L h^{-1}): **a** Ca^{2+}, **b** Mg^{2+}, **c** SO_4^{2-}

Fouling phenomena did not depend on the type of membrane (NF or RO), but rather on water permeability level. As RO membranes are dense membranes, irreversible fouling probably develops on the outer surface of all the membranes tested. A more efficient pre-treatment would not solve fouling problems as shown by Reimann (2002) for an equivalent effluent (low-contaminated washing water for carrots): with ultrafiltration with a 0.1-µm or 0.05-µm pore diameter as pre-treatment, a loss of permeate flux during the first two hours of RO treatment was also observed.

Both concentration polarization and fouling phenomena may have either beneficial or detrimental impacts on membrane selectivity (Aimar et al. 2010). Consequently, membrane performances were compared before and after the critical flux.

Sorption phenomena

Adsorption can increase with polarization concentration and impact fouling (Aimar et al. 2016). To assess sorption phenomena, an experiment was run on the LabStak M20 device equipped with 3 pairs of membranes (total filtration area = 0.108 m^2) and without TMP (TMP = 0 bar). The initial volume in the tank was 28.1 L. Samples were taken in the tank at the beginning and after 30 min of operation, when equilibrium was expected to be reached. As expected for a microfiltrated solution, there is no more difference between total and dissolved COD. Results (Table 6) show a loss of fructose, glucose and sucrose of, respectively, 5 mg L^{-1}, 4.8 mg L^{-1} and 23 mg L^{-1}, probably due to adsorption on the membranes. It corresponds to a calculated COD_{sugars} loss of 36 mg O_2 L^{-1}

t7.1 **Table 7** Comparison of pH in the permeate and retentate of NF membranes

t7.2		SR3D pH in		DK pH in		NF270 pH in		NFW pH in	
t7.3		Permeate	Retentate	Permeate	Retentate	Permeate	Retentate	Permeate	Retentate
t7.4	5 bar	7.1	7.5	7.5	7.4	7.3	7.4	7.4	7.4
t7.5	10 bar	6.4	7.6	7.3	7.5	7.3	7.5	7.2	7.5
t7.6	15 bar	6.2	7.5	7.5	7.4	7.2	7.3	7.3	7.3
t7.7	20 bar	6.8	7.5	7.6	7.6	7.4	7.6	7.6	7.6
t7.8	30 bar	6.1	7.5	7.4	7.4	7.4	7.5	7.3	7.4

t8.1 **Table 8** Comparison of CH in the permeate of NF membranes

t8.2		SR3D CH in °f	DK CH in °f	NF270 CH in °f	NFW CH in °f
t8.3	5 bar	3.3	3.8	3.2	4.8
t8.4	10 bar	< 2	2.2	2.4	4.3
t8.5	15 bar	< 2	2.2	2.1	4.1
t8.6	20 bar	< 2	2.9	3.5	4.0
t8.7	30 bar	< 2	2.2	4.0	4.6

while COD loss is about 88 mg O_2 L^{-1}, showing that other molecules (equivalent to a COD_{diff} of about 52 mg O_2 L^{-1}) such as peptides are also adsorbed on the membranes. Actually, proteins have a strong tendency to adsorb on membranes (Aimar et al. 2016). The quantity adsorbed is about 1.3 g m^{-2} for fructose, 1.3 g m^{-2} for glucose and 6 g m^{-2} for sucrose. Such adsorption had already been observed by Nguyen et al. (2016) for glucose, but at a lower level.

No significant discrepancy is noticed in ion concentrations before and after contact with the membranes.

COD and sugar rejection

The rejection of COD and sugars versus permeate flux for NF membranes is given in Fig. 8. They increase with the solute MW and decrease with the MWCO of the membrane (Table 2) indicating that size exclusion is the major mechanism for the studied solutes tested on these membranes. This conclusion is consistent with other studies (Mohammad et al. 2010; Nguyen et al. 2015).

The maximal COD rejections for the DK (150–300 g mol^{-1}), NF270 (150–300 g mol^{-1}), SR3D (200 g mol^{-1}) and NFW (300–500 g mol^{-1}) membranes are, respectively, 95.8%, 94.9%, 92.1% and 82.8% (Fig. 8a) and correspond to minimal COD values in the permeate of, respectively, 20, 25, 48 and 82 mg O_2 L^{-1}. The same membrane ranking is observed with sugars (Fig. 8b, c), the most rejected being sucrose, which has the highest MW. Due to their equivalent chemical structure, MW and Stokes diameter, there is no significant difference between glucose and fructose in terms of rejection, whatever the membrane. Nevertheless, glucose rejection is always slightly higher than that of fructose. Such phenomena had already been observed between two C5 sugars and attributed to hydration differences (Galema and Hoeiland 1991; Hua et al. 2010; Nguyen et al. 2015). It could also be explained by differences in the interaction energy with the membrane, as suggested by Yao et al. (2018) for the rejection of monosaccharides in NF membranes.

It is also observed that rejections decrease when the permeate flux increases above the critical flux (between 80 and 100 L h^{-1} m^{-2} for all the membranes), as already noticed to a lesser extent for glucose in a model mixture by Nguyen et al. (2015) with the NF270 membrane and for the highest flux (above 150 L h^{-1} m^{-2}). To the contrary, Almazán et al. (2015) who studied glucose behaviour alone in solution observed a stabilization of its rejection for increasing pressure and for different membranes including DK. Then, for a complex solution such as carrot-peeling wastewater, working above the critical flux has a negative impact on the rejection of sugars.

Regarding RO, whatever the membrane, the permeates contain between 10 and 17 mg O_2 L^{-1} corresponding to a COD rejection of about 97.2% ± 0.9% (figure not shown). At the same time, fructose, glucose and sucrose rejections are about 99.2% ± 0.5%. Whatever the pressure, COD and the rejection of sugars are always high due to a predominant

t9.1 **Table 9** Example of ion mass balance: DK membrane at 5 bar

	Concentration in permeate (mmol L^{-1})	Concentration in retentate (mmol L^{-1})	Rejection
Cl^-	0,89	1.35	34%
NO_3^-	0.08	0.10	20%
PO_4^{3-}	0.00	0.02	100%
SO_4^{2-}	0.00	0.18	100%
HCO_3^-	0.38	0.82	54%
Negatively charged ions	*1.35*	*2.69*	
Na^+	0.57	0.82	31%
K^+	0.58	0.91	36%
Mg^{2+}	0.03	0.24	86%
Ca^{2+}	0.24	0.94	74%
H^+	Negligible	Negligible	–
Positively charged ions	*1.69*	*4.09*	
Missing negatively charged ions	*0.34*	*1.4*	*76%*

t10.1 **Table 10** The principal amino acids in carrots and their properties

t10.2 Amino acid	Value in carrot (as per USDA)	Isoelectric point	Solubility in water at 25 °C	MW	Charge at neutral pH
t10.3 Glutamic acid	0.366 g/100 g	3.22	0.9 g/100 g	147.1 g mol^{-1}	*Negative*
t10.4 Threonine	0.191 g/100 g	5.87	9.1 g/100 g	119.1 g mol^{-1}	≈ Neutral
t10.5 Aspartic acid	0.190 g/100 g	2.77	0.5 g/100 g	133.1 g mol^{-1}	*Negative*
t10.6 Alanine	0.113 g/100 g	6.01	16.7 g/100 g	89.1 g mol^{-1}	≈ Neutral
t10.7 Leucine	0.102 g/100 g	5.98	2.4 g/100 g	131.2 g mol^{-1}	≈ Neutral
t10.8 Lysine	0.101 g/100 g	9.74	0.6 g/100 g	146.2 g mol^{-1}	*Positive*

size exclusion effect. This is consistent with other studies on sugars, always rejected at more than 95% (Nguyen et al. 2015). Given this high rejection range, no difference can be made between sucrose and C6 sugars, and a fortiori between glucose and fructose.

The fact that the rejection of COD is always inferior to the rejection of sugars suggests that additional (and not quantified) organic solutes in the solution pass through the membrane more easily than sugars. This is confirmed by the calculation of COD_{diff} rejection for two NF (DK and NFW) (Fig. 9a) and two RO (BW30 and ESPA4) membranes (Fig. 9b). It appears always slightly below COD rejection, confirming that these solutes are less rejected than sugars. For treatment with ESPA4, OD_{215} rejection was only about 92% ± 3%, similar to COD_{diff} rejection showing that these solutes could be amino acids.

Rejection of minerals

Rejections of monovalent and divalent ions are presented separately. Due to their quasi absence in the raw wastewater (Table 3), nitrate (NO_3^-) and ammonium (NH_4^+) rejection figures are not presented, as is the case for the only trivalent ion detected (PO_4^{3-}), which is always 100% rejected regardless of membrane type.

Figure 10 shows rejections obtained for monovalent ions (Na^+, K^+, Cl^-) with the four NF membranes. The rejection order between the membranes is in accordance with $MgSO_4$ rejection indicated by manufacturers (Table 2): higher for SR3D ($MgSO_4$ rejection > 99%) followed by DK ($MgSO_4$ rejection 98%), NF270 ($MgSO_4$ rejection 97%) and NFW ($MgSO_4$ rejection 97%). The same tendency was observed for divalent ions (Ca^{2+}, Mg^{2+}, SO_4^{2-}) in Fig. 11. An exception

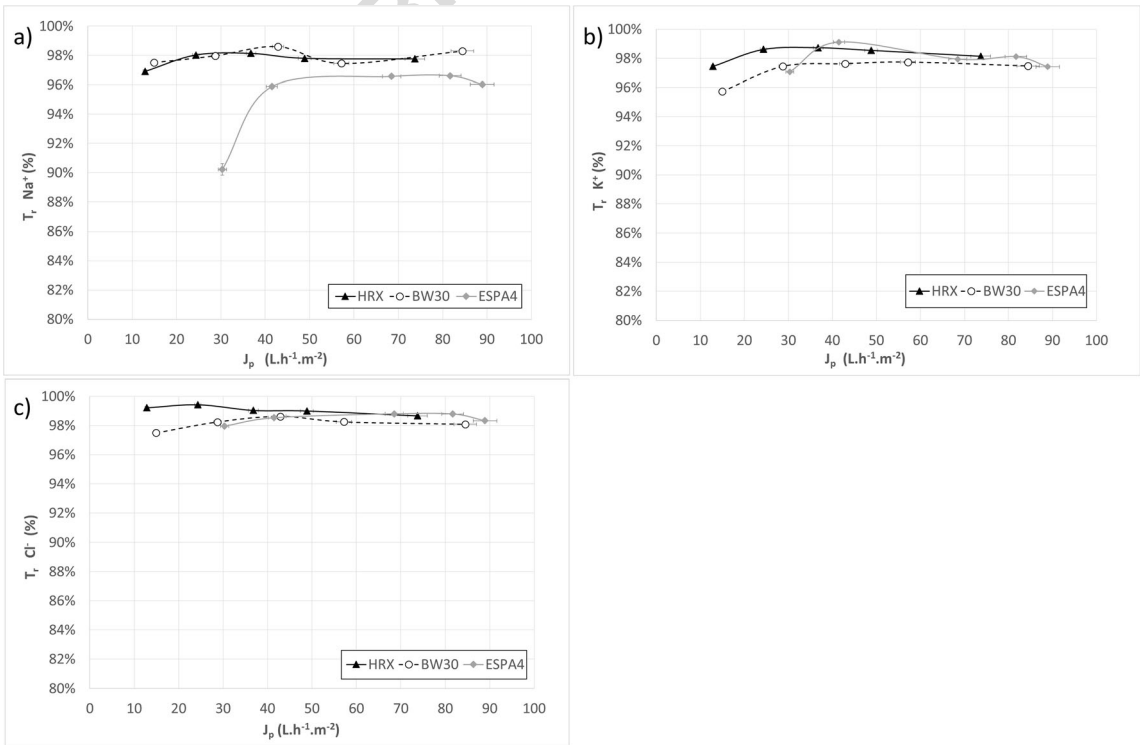

Fig. 12 Monovalent ion rejection as a function of permeate flux with RO membranes (20 °C, feed flow rate = 300 L h^{-1}): **a** Na^+, **b** K^+, **c** Cl^-

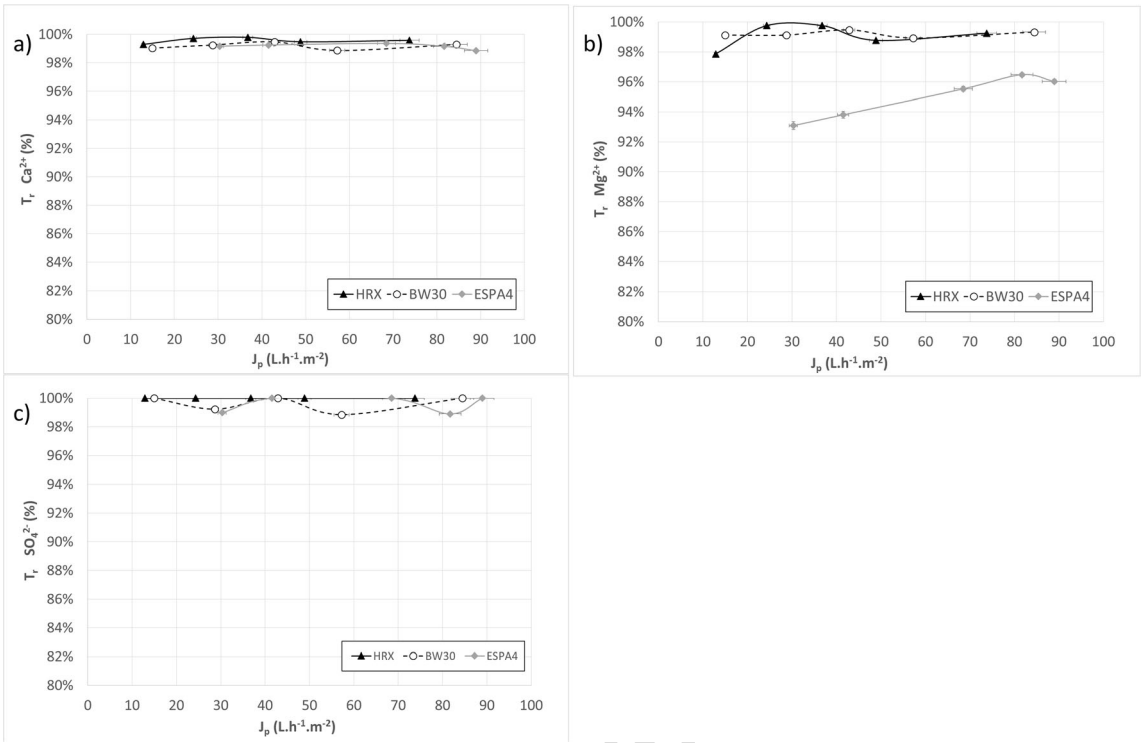

Fig. 13 Divalent ion rejection as a function of permeate flux with RO membranes (20 °C, feed flow rate = 300 L h^{-1}): **a** Ca^{2+}, **b** Mg^{2+}, **c** SO_4^{2-}

was observed with the SR3D membrane for magnesium (Fig. 11b) and sulphates (Fig. 11c), highlighting a different behaviour for this membrane. This is consistent with the measures of pH (Table 7), CH (Table 8) and OD_{215} of the permeate: indeed, pH and CH are much lower as compared with other membranes, suggesting a higher migration of protons and a lower migration of bicarbonates (HCO_3^-, major form at neutral pH). At the same time, OD_{215} rejection is smaller, at 31% ± 9% showing that the transfer of amino acid-type molecules though this membrane is much higher.

The rejections of monovalent ions (Na^+, K^+, Cl^-) (Fig. 10) were globally lower than those for divalent ions (Ca^{2+}, Mg^{2+}, SO_4^{2-}) (Fig. 11) and lower than those for the trivalent PO_4^{3-} (100%). As an example, rejection rates for Na^+ and Mg^{2+} (40% and > 90% respectively) are very different for DK membrane at 60 L h^{-1} m^{-2}, although they have similar MW. This is consistent with the Donnan space charge model (Aimar 2006). For SO_4^{2-} and PO_4^{3-}, with higher, similar molecular weights (about 95 g mol^{-1}), the size effect is of major importance on their rejection, which moreover is not affected by the flux (no decrease above the critical flux).

Rejection values for sulphates were 100% for DK and NF270, 97.2% for NFW and 96.3% for SR3D, consistent with manufacturers' data (Table 2) with the exception again of SR3D which displays lesser sulphate rejection than expected, perhaps balanced by higher bicarbonate rejection, as noticed above. Regarding magnesium, for all the membranes, the maximal rejections are significantly lower than expected: 93.6% for DK, 82.0% for NF270, 59.3% for NFW and 88.4% for SR3D. This could be explained by the presence in the effluent of additional non-qualified small negatively charged molecules. Indeed, the ionic mass balance indicates that the sum of the negatively charged ions is lower than that of the positively charged ion charges (example for the DK membrane at 5 bar in Table 9). This difference is greater for the retentate, showing that those negatively charged molecules are well retained (76%). As shown previously (OD at about 215 nm), the presence in wastewater of amino acids such as glutamic acid, aspartic acid and lysine is suspected. Being negatively charged at neutral pH (Table 10), they would transfer together with cationic molecules or minerals, such as magnesium ions, to ensure electroneutrality, which might explain its unexpected lower presence.

Table 11 Maximal sodium (Na^+) and chloride (Cl^-) rejections with membranes

		HRX	BW30	ESPA4
This study	Na^+ rejections	98.1% (rank 2)	98.6% (rank 1)	96.6% (rank 3)
	Cl^- rejections	99.4% (rank 1)	98.6% (rank 3)	98.8% (rank 2)
Manufacturers' data		99.6% (rank 1)	99.5% (rank 2)	99.2% (rank 3)

t12.1 **Table 12** Permeate quality of
t12.2 selected membranes for recycling

		NF270 (NF)	DK (NF)	ESPA4 (RO)	
t12.3	Optimum TMP (bars)	15.5	15.5	9.7	14.8
t12.4	J_p (L h^{-1} m^{-2})	104	64	41	68
t12.5	Total COD (mg O_2 L^{-1})	25	21	14	12
t12.6	Conductivity (μS cm^{-1})	195	134	9	8
t12.7	pH	7.2	7.4	6.1	5.8
t12.8	CH (°f)	2.1	2.2	< 2	< 2
t12.9	Fructose (mg L^{-1})	3	2	< 1	< 1
t12.10	Glucose (mg L^{-1})	3	2	< 1	< 1
t12.11	Sucrose (mg L^{-1})	2	2	3	2
t12.12	Cl^- (mg L^{-1})	30	22	< 1	< 1
t12.13	NO_3^- (mg L^{-1})	6	4	< 1	< 1
t12.14	PO_4^{3-} (mg L^{-1})	< 1	< 1	< 1	< 1
t12.15	SO_4^{2-} (mg L^{-1})	< 1	< 1	< 1	< 1
t12.16	Na^+ (mg L^{-1})	12	11	< 1	< 1
t12.17	K^+(mg L^{-1})	20	17	< 1	1
t12.18	Mg^{2+} (mg L^{-1})	1	< 1	< 1	< 1
t12.19	Ca^{2+} (mg L^{-1})	12	5	< 1	< 1
t12.20	OD 254 nm	n.d.	n.d.	0.015	0.005
t12.21	Colour (*L*/*a*/*b*)	n.d.	n.d.	99.1/0.1/0.4	100.1/0/0

n.d. not determined

Concerning ion rejections with RO membranes, results obtained with the ESPA4, HRX and BW30 membranes are compared in Fig. 12 and Fig. 13. The membranes' ranking generally conforms to the manufacturer's data (Table 11) with rejections higher than 96% in most cases. Surprisingly, the ESPA4 membrane gives better rejections than indicated, especially for the major salts in solution (Cl^-, Ca^{2+}, K^+). As for the NF membranes and for the same reason, cations are less retained than anions by RO membranes.

Choice of NF or RO membranes for the reconditioning treatment

Amongst NF membranes, the NF270 at TMP = 15 bar appears as the best compromise in terms of COD rejection and permeate flux. Nevertheless, at this pressure, the permeate flux is above the critical value which increases cleaning constraints. The DK membrane at the same TMP allows the same COD rejection to be obtained, but with a permeate flux below the critical flux. The corresponding permeate qualities are summarized in Table 12.

For RO membranes, considering that COD rejection is not a relevant criterion here, the choice may be driven by the permeate productivity, and consequently the highest water permeability (Table 5). In that case, ESPA4 appears as the best choice, even more so it operates below the critical flux (TMP < 15 bar). The permeate quality with this membrane at a TMP of 10 and 15 bar is summarized in Table 12 and corresponds to rejections up to 98.3, 98.0, 99.2, 99.2 and 99.4% in conductivity, COD, fructose, glucose and sucrose, respectively.

For the same operating pressure (TMP = 15 bar), the permeate produced with ESPA4 seems to most closely match the quality criteria for drinking water, with a much lower organic matter content (COD) especially, as compared with DK and NF270. Moreover, it has a similar productivity to DK. For these reasons, and in order to have the best COD rejection while limiting the fouling risks, ESPA4 can be selected for complementary tests on a pre-industrial pilot scale. However, with the RO membrane's high conductivity rejection, particular attention would have to be paid to the calco-carbonic balance of the water produced in order to avoid corrosion.

Conclusions

The production of water of sufficient quality for reuse in the vegetable industry was studied in the specific case of a complex carrot-peeling effluent. A pre-treatment consisting of double sieving steps at 169 μm and 79 μm, followed by a 0.5-μm microfiltration, was necessary to eliminate larger particles and minimize fouling issues for subsequent treatment steps. High-quality water with low conductivity (< 8 μS cm^{-1}), low COD (< 12 mg O_2 L^{-1}) and low sugar content (< 4 mg L^{-1}) can be obtained by reverse osmosis treatment with the ESPA4 membrane (Hydranautics-Nitto Group

Company). As wastewater from blanching operations contains the same components as peeling wastewater, similar treatment could be considered and performances predicted. They allow for serious consideration of the possibility of water reuse in vegetable processing plants, prior to the blanching step which can act as a thermal barrier and further contribute to microbiological safety. However, water treated by reverse osmosis is demineralized, disrupting the calco-carbonic equilibrium and thus increasing the risks of corrosion. These issues remain to be studied on an industrial scale.

Acknowledgements This research was supported by the French National Agency for Research (ANR) through the MINIMEAU Project (ANR-17-CE10-0015). The authors wish to thank Mélanie Biland and Saïda Maaref for their valuable contributions to this work. The CTCPA (Paris, France) is acknowledged for sharing its expertise in vegetable industries and for providing the industrial partner for the effluent supply.

References

Aimar P (2006) Filtration membranaire (OI, NF, UF) Mise en œuvre et performances. In: Procédés de traitement des eaux potables, industrielles et urbaines, base documentaire : TIB318DUO(ref. article : w4110). Ed. Techniques de l'Ingénieur, St-Denis, France

Aimar P, Bacchin P, Maurel A (2010) Filtration membranaire (OI, NF, UF, MFT) Aspects théoriques : perméabilité et sélectivité. In: Opérations unitaires : techniques séparatives sur membranes, base documentaire : TIB331DUO(ref. article : j2790). Ed. Techniques de l'Ingénieur, St-Denis, France

Aimar P, Bacchin P, Maurel A (2016) Filtration membranaire (OI, NF, UF, MFT) Aspects théoriques : mécanismes de transfert. In: Opérations unitaires : techniques séparatives sur membranes, base documentaire : TIB331DUO(ref. article : j2789). Ed. Techniques de l'Ingénieur, St-Denis, France

Almazán JE, Romero-Dondiz EM, Rajal VB, Castro-Vidaurre EF (2015) Nanofiltration of glucose: analysis of parameters and membrane characterization. Chem Eng Res Des 94:485–493

Ardley S, Arnold P, Younker J, Rand J (2019) Wastewater characterization and treatment at a blueberry and carrot processing plant. Water Resour Ind 21:100–107

ASTM D4189–07 (2014) Standard test method for silt density index (SDI) of water

Bacchin P, Aimar P, Field RW (2006) Critical and sustainable fluxes: theory, experiments and applications. J Membr Sci 281(1–2):42–69

Balannec B, Vourch M, Rabiller-Baudry M, Chaufer B (2005) Comparative study of different nanofiltration and reverse osmosis membranes for dairy effluent treatment by dead-end filtration. Sep Pur Technol 42(2):195–200. https://doi.org/10.1016/j.seppur.2004.07.013

Casani S, Rouhany M, Knochel S (2005) A discussion paper on challenges and limitations to water reuse and hygiene in the food industry. Water Res 39(6):1134–1146. https://doi.org/10.1016/j.watres.2004.12.015

European Union (2018) Best available technique (BAT) - reference document in the food, drink and milk industries

Galema SA, Hoeiland H (1991) Stereochemical aspects of hydration of carbohydrates in aqueous solutions. 3. Density and ultrasound measurements. J Phys Chem 95(13):5321–5326

Galier S, Savignac J, Roux-de Balmann H (2013) Influence of the ionic composition on the diffusion mass transfer of saccharides through a cation-exchange membrane. Sep Pur Technol 109:1–8

Garnier C, Guiga W, Lameloise ML, Degrand L, Fargues C (2019) Tools development for water recycling. In: 9th IWA membrane technology conference (Toulouse)

Hua X, Zhao H, Yang R, Zhang W, Zhao W (2010) Coupled model of extended Nernst–Planck equation and film theory in nanofiltration for xylo-oligosaccharide syrup. J Food Eng 100(2):302–309

Kern J, Reimann W, Schlüter O (2006) Treatment of recycled carrot washing water. Environ Technol 27(4):459–466

Klemes J, Smith R, Kim JK (2008) Preface. In: Klemes J, Smith R, Kim JK (eds) Handbook of water and energy management in food processing. Woodhead Publ ltd, Cambridge, pp XXV–XXXVIII

Lehto M, Sipilä I, Sorvala S, Hellstedt M, Kymäläinen HR, Sjöberg AM (2009) Evaluation of on-farm biological treatment processes for wastewaters from vegetable peeling. Environ Technol 30(1):3–10

Lehto M, Sipilä I, Alakukku L, Kymalainen HR (2014) Water consumption and wastewaters in fresh-cut vegetable production. Agric Food Sci 23(4):246–256. https://doi.org/10.23986/afsci.41306

Lens PNL, Hulshoff Pol LW, Wilderer P, Asano T (2002) Water recycling and resource recovery in industry: analysis, technologies and implementation. IWA, London

Macedo EA (2005) Solubility of amino acids, sugars, and proteins. Pure Appl Chem 77(3):559–568

Manzocco L, Ignat A, Anese M, Bot F, Calligaris S, Valoppi F, Nicoli MC (2015) Efficient management of the water resource in the fresh-cut industry: current status and perspectives. Trends Food Sci Technol 46(2):286–294. https://doi.org/10.1016/j.tifs.2015.09.003

Mohammad AW, Basha RK, Leo C (2010) Nanofiltration of glucose solution containing salts: effects of membrane characteristics, organic component and salts on retention. J Food Eng 97(4):510–518

Mundi G (2013) Assessment of effective solids removal technologies to determine potential for vegetable washwater reuse, Master Thesis of Applied Science In Engineering, Univ. Guelph, Ontario, Canada - November, 2013

Mundi GS, Zytner RG (2015) Effective solid removal technologies for wash-water treatment to allow water reuse in the fresh-cut fruit and vegetable industry. J Agric Sci Technol A 5:396–407

Negaresh E, Antony A, Bassandeh M, Richardson DE, Leslie G (2012) Selective separation of contaminants from paper mill effluent using nanofiltration. Chem Eng Res Des 90(4):576–583

Nelson H, Singh R, Toledo R, Singh N (2007) The use of a submerged microfiltration system for regeneration and reuse of wastewater in a fresh-cut vegetable operation. Sep Sci Technol 42(11):2473–2481. https://doi.org/10.1080/01496390701477147

Nemati-Amirkolaii K, Romdhana H, Lameloise ML (2019) Pinch methods for efficient use of water in food industry: a survey review. Sustainability 11:4492

NF EN 872 - https://norminfo.afnor.org/norme/NF%20EN%20872/qualite-de-leau-dosage-des-matieres-en-suspension-methode-par-filtration-sur-filtre-en-fibres-de-verre/70297

Nguyen N, Fargues C, Guiga W, Lameloise ML (2015) Assessing nanofiltration and reverse osmosis for the detoxification of lignocellulosic hydrolysates. J Membr Sci 487:40–50

Nguyen DTNN, Lameloise ML, Guiga W, Lewandowski R, Bouix M, Fargues C (2016) Optimization and modeling of dianonfiltration process for the detoxification of ligno-cellulosic hydrolysates-study at pre-industrial scale. J Membr Sci 512:111–121

Racar M, Dolar D, Špehar A, Košutić K (2017) Application of UF/NF/RO membranes for treatment and reuse of rendering plant wastewater. Process Saf Environ Prot 105:386–392

Reimann W (2002) Treatment of agricultural wastewater and reuse. Water Sci Technol 46(11–12):177–182

Richards LA, Vuachère M, Schäfer AI (2010) Impact of pH on the removal of fluoride, nitrate and boron by nanofiltration/reverse osmosis. Desalination 261(3):331–337

Sagne C, Fargues C, Lewandowski R, Lameloise ML, Decloux M (2008) Screening of reverse osmosis membranes for the treatment and reuse

of distillery condensates into alcoholic fermentation. Desalination 219(1–3):335–347

Sharma KD, Karki S, Thakur NS, Attri S (2012) Chemical composition, functional properties and processing of carrot—a review. J Food Sci Technol 49(1):22–32

Siddiq M, Uebersax MA (2018) Handbook of vegetables and vegetable processing. Wiley Online Library

Truc A (2007) Traitements tertiaires des effluents industriels. In: Technologies de l'eau 3(G1310). Ed. Techniques de l'Ingénieur, St-Denis, France

Valta K, Moustakas K, Sotiropoulos A, Malamis D, Haralambous KJ (2016) Adaptation measures for the food and beverage industry to the impact of climate change on water availability. Desalin Water Treat 57(5):2336–2343. https://doi.org/10.1080/19443994.2015.1049407

Warsinger DM, Chakraborty S, Tow EW, Plumlee MH, Bellona C, Loutatidou S, Karimi L, Mikelonis AM, Achilli A, Ghassemi A, Padhye LP, Snyder SA, Curcio S, Vecitis CD, Arafat HA, Lienhard JH V (2018) A review of polymeric membranes and processes for potable water reuse. Prog Polymer Sci 81:209–237

Yao L, Qin Z, Chen Q, Zhao M, Zhao H, Ahmad W, Fan L, Zhao L (2018) Insights into the nanofiltration separation mechanism of monosaccharides by molecular dynamics simulation. Sep Pur Technol 205:48–57

Yuan J, Duan J, Saint CP, Mulcahy D (2018) Removal of glyphosate and aminomethylphosphonic acid from synthetic water by nanofiltration. Environ Technol 39(11):1384–1392. https://doi.org/10.1080/09593330.2017.1329356

Zhao F, Xu K, Ren H, Ding L, Geng J, Zhang Y (2015) Combined effects of organic matter and calcium on biofouling of nanofiltration membranes. J Membr Sci 486:177–188